For publication in *ACC 2018*

Building Energy Disaggregation using Spatiotemporal Pattern Network

Chao Liu[a] Zhanhong Jiang[a] Adedotun Akintayo[a] Gregor P. Henze[b,c] Soumik Sarkar[a]
cliu5@tsinghua.edu.cn, zhjiang@iastate.edu, akintayo@iastate.edu
gregor.henze@colorado.edu, soumiks@iastate.edu
[a]Department of Mechanical Engineering, Iowa State University, Ames, IA 50011, USA
[b]Department of Civil, Environmental and Architectural Engineering,
University of Colorado, Boulder, CO 80309, USA
[c]National Renewable Energy Laboratory, Golden, CO 80401,USA

***Abstract*— Numerous studies on non-intrusive load monitoring (NILM) of electrical demand have been performed for the purpose of identifying load components only using univariate data, such as the identification of a certain type of end-use (e.g., lighting load) via whole building electricity consumption time series. However, additional time series data may become useful in providing distinguishable features for energy disaggregation which can be rendered as a multivariate time series data analysis problem. This paper presents a novel probabilistic graphical modeling approach called the spatiotemporal pattern network (STPN) for addressing such problem of pattern extraction from multivariate time-series data with application to building energy disaggregation. The proposed scheme shows promise in dealing with multivariate time-series with widely different characteristics for the improvement in energy disaggregation performance. We use multiple real data sets to validate the STPN framework along with performance comparison with the state-of-the-art techniques such as factorial hidden Markov models (FHMM) and combinatorial optimization (CO).**

1. Introduction

Non-intrusive load monitoring is a well studied problem involving disaggregation of the total electrical energy consumption of a building into its constituent electric load components without the need for extensive metering installations on individual end-uses. Such problems are relevant and challenging from the perspective of software-based detection for control of end-use patterns as well as the future internet of things (IoT). [1] presented an overview of load disaggregation concepts which began from the pioneering disaggregation technique in [1] that detected sharp changes in signals to optimization of error terms for pattern detection using genetic algorithms [2]. In [3], Fourier transforms was used to categorize the useful patterns of end-use signals. Moreover, authors in [3] evaluated the performance of factorial hidden Markov models (FHMM)[4] for the energy disaggregation problem. With the importance of NILM, arose the need for standardized datasets for benchmarking the large variety of published algorithms. In that light, authors of [5] established accordingly the Reference Energy Disaggregation Data set (REDD), facilitated by hardware and software systems designed to collect real and reactive power of appliances from multiple homes in Boston, MA in 2011. NILMTK, an open source toolkit was subsequently developed [6] as a common platform to enhance the reproducibility of the algorithms' results on available datasets such as REDD [5], BLUED [7], Smart* [8], and several others. In order to benchmark the results of the algorithms, several performance evaluation metrics were proposed [9], [10], [11]. Previous work on NILM for energy disaggregation has been primarily based on univariate real power measurements at different sampling intervals [12], [13], [14], [15], [16], [17], [18]. However, a univariate measurement is possibly insufficient for the task of identifying the dominant load contributions such as air-conditioning related demand.

In this context, a recently developed framework of spatiotemporal pattern networks (STPN) that is built on the concept of symbolic dynamics is applied to NILM. STPN is proposed to model multivariate time series, via learning atomic patterns (APs, Markov models for individual variables) and relational patterns (RPs, Markov models to model causal interactions between variables) [19], [20], [21]. Patterns of multivariate time series data are formed based on these features (APs and RPs) and then used to study the characteristics of electricity usage. This paper also applies a mutual information based metric to explore the energy consumption patterns and selects the most valuable variables for disaggregation. Diverse test cases are used for validation showing that it outperforms the state-of-the-art techniques in NILM.

Outline: The remaining paper is organized as follows. Section 2 provides a brief background and preliminaries of STPN. Section 3 presents the framework of energy disaggregation using multivariate time-series data via STPN. Section 4 describes results for disaggregation using RBSAM data set. Finally, the paper is summarized and concluded in Section 5.

2. Background on Spatiotemporal Pattern Network (STPN)

This section presents the background and some preliminaries on STPN for characterizing the proposed methodology. Before introducing STPN, the concept of probabilistic finite

state automaton (PFSA) is first defined here as a basis. PFSA is defined in the symbolic space that is generated via time series abstraction (preprocessing and discretization/partitioning). As shown in Fig. 1, the time-series data is discretized into symbol sequences and then state sequences, PFSA is formed using D-Markov machine. More formally, based on a deterministic finite state automaton (DFSA) $\mathcal{D} = (S, Q, \chi)$, a PFSA, an extension to probabilistic setting from DFSA is defined as a pair $\mathcal{P} = (\mathcal{D}, \psi)$, i.e., the PFSA is a 4-tuple $\mathcal{P} = (S, Q, \chi, \psi)$, where:

1) S is a set of finite size for the symbol alphabet and $S \neq \emptyset$;
2) Q is a set of finite size for states and $Q \neq \emptyset$;
3) $\chi : Q \times S \to Q$ is the mapping for state transition;
4) $\psi : Q \times S \to [0, 1]$ is defined as a symbol generation function, i.e., probability morph function which is such that $\sum_{\sigma \in S} \psi(q, \sigma) = 1 \quad \forall q \in Q$, where p_{ij} indicates the probability of the symbol $\sigma_j \in S$ occurring with the state $q_i \in Q$.

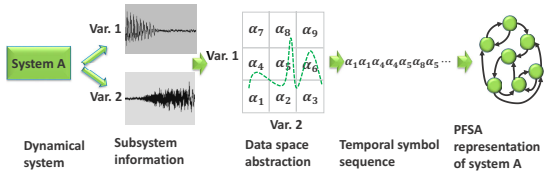

Fig. 1. *Steps to form a PFSA model with time-series data*

Using the xD-Markov machine defined in [22], a PFSA can be used to explore the relationship of two time-series data as shown in Fig. 2. Let the symbolic system a represent a measurement at the aggregate side (metering data) and symbolic system b represent an end-use i (sub-metering data), the transition matrix Ω^{ab} (relational pattern, RP) is used to characterize features in the total energy consumption due to the end-use i. Atomic pattern (AP) is also shown here that is used to capture the predictability of end-use i based on its past measurements. The metric Λ^{ab} for the patterns (APs and RPs) is used to evaluate the importance of the patterns.

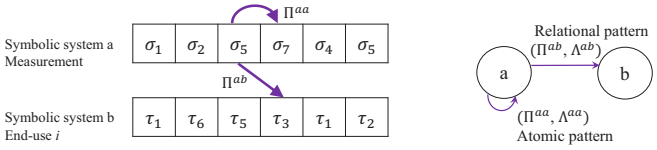

Fig. 2. *Extraction of atomic patterns and relational patterns (with D-Markov machine and xD-Markov machine respectively and $D = 1$ for simplicity, i.e., states and symbols are equivalent) to model individual variables and interaction among different variables respectively.*

With the description of PFSA, D-Markov machine, and xD-Markov machine [23], STPN is defined in as follows[20].

Definition. A PFSA based STPN is a 4-tuple $W_D \equiv (Q^a, \Sigma^b, \Omega^{ab}, \Lambda^{ab})$: (a, b denote nodes of the STPN) (a)

1) $Q^a = \{q_1, q_2, \cdots, q_{|Q^a|}\}$ is the state set corresponding to symbol sequences S^a;
2) $\Sigma^b = \{\sigma_0, \cdots, \sigma_{|\Sigma^b|-1}\}$ is the alphabet set of symbol sequence S^b;
3) Ω^{ab} is the symbol generation matrix of size $|Q^a| \times |\Sigma^b|$, the ij^{th} element of Π^{ab} denotes the probability of finding the symbol σ_j in the symbol string s^b while making a transition from the state q_i in the symbol sequence S^a; while self-symbol generation matrices are called atomic patterns (APs) i.e., when $a = b$, cross-symbol generation matrices are called relational patterns (RPs) i.e., when $a \neq b$.
4) Λ^{ab} denotes a metric that can represent the importance of the learnt pattern for $a \to b$ which is a function of Π^{ab}.

3. STPN FRAMEWORK FOR NILM WITH MULTIVARIATE MEASUREMENTS

While the previous section applies STPN in exploring patterns in different end-uses, here we introduce the STPN framework for energy disaggregation using multivariate time-series data. Let us denote $\mathbf{X} = \{X^{\mathbb{A}}(t),\ t \in \mathbb{N},\ \mathbb{A} = 1, 2, \cdots, f\}$ for both kinds of multivariate time-series data in a home, and $\mathbf{Y} = \{Y^{\mathbb{B}}(t),\ t \in \mathbb{N}, \mathbb{B} = 1, 2, \cdots, g\}$ for the power consumption for the end-uses. f is the number of time series at the aggregate side, g is the number of end-uses.

For the time-series $\mathbf{X}$ and $\mathbf{Y}$, symbol sequences $\boldsymbol{\sigma} = \{\sigma^{\mathbb{A}}(t)\}$ and $\boldsymbol{\tau} = \{\tau^{\mathbb{B}}(t)\}$ can be obtained after data processing and partitioning. To form an STPN for disaggregation, joint symbol sequences $\sigma^J = \sigma^1(t) \oplus \cdots \oplus \sigma^f(t)$ and $\tau^J = \tau^1(t) \oplus \cdots \oplus \tau^g(t)$ are formed based on the symbol sequences $\boldsymbol{\sigma}$ and $\boldsymbol{\tau}$ respectively. Note, the joint symbol space is generated via the direct sum of the individual symbol spaces. For example, the direct sum $\sigma^a \oplus \sigma^b$ defines the product space of σ^a and σ^b. Here, we use the depth $D = 1$, which means the symbol and the state are equivalent. Then we can have the state sequences Φ and Ψ generated from the joint symbols sequences respectively.

With the setup, the learning stage of STPN is to compute the transition matrix $\boldsymbol{\Omega}(\Phi, \boldsymbol{\tau^J})$ from the states in Φ to the symbols in $\boldsymbol{\tau^J}$ using a frequentist's approach (e.g. counting the number of occurrences). For example, the probability of the state Φ_m to the symbol τ_n^J can be computed by $Pr(\phi_m, \tau_n^J) = N_{mn}/N_m$, where N_{mn} is the number of times that the symbol $\tau_n^J \in \boldsymbol{\tau^J}$ is emanated after the state $\phi_m \in \Phi$, i.e.,

$$N_{mn} \triangleq |\{(\phi(k), \tau^J(k+1)) : \tau^J(k+1) = \tau_n^J \mid \phi(k) = \phi_m\}|,$$
$$m = 1, 2, \cdots, \prod_{\mathbb{A}=1}^{f} |\sigma^{\mathbb{A}}|, \quad n = 1, 2, \cdots, \prod_{\mathbb{B}=1}^{g} |\tau^{\mathbb{B}}|, \tag{1}$$

where $\phi(k)$ is the k^{th} state in the state sequence Φ and $\tau^J(k+1)$ is the $(k+1)^{th}$ symbol in the symbol sequence

$\boldsymbol{\tau^J}$. The time lag equals to 1 in this case, and $N_m \triangleq \sum_{n=1}^{\prod_{\mathbb{B}=1}^{g}|\tau^{\mathbb{B}}|} N_{mn}$.

The real values represented by the symbols $\boldsymbol{\tau^J}$ can be also computed from the training data, and noted as $E\big(\mathbf{Y}|\tau^J = n\big), n = 1, 2, \cdots, \prod_{\mathbb{B}=1}^{g}|\tau^{\mathbb{B}}|$. In the disaggregation stage, only the time-series $\tilde{\mathbf{X}}$ is known, the time-series of end-uses $\tilde{\mathbf{Y}}$ is assumed unknown and used for testing. Similarly, the symbol sequences $\tilde{\boldsymbol{\sigma}}$ and joint symbol sequence σ^J are obtained after partitioning, and the corresponding state sequences are generated using D-Markov and xD-Markov machines. Then the power consumptions of the end-uses $\mathbf{Y}_s$ are obtained, $\mathbf{Y}_s = \sum_{n=1}^{\prod_{\mathbb{B}=1}^{g}|\tau^{\mathbb{B}}|} Pr(\tau^J|\tilde{\phi}(t)) \cdot E\big(\mathbf{Y}|\tau^J = n\big)$.

With multivariate time-series data, the disaggregation formed in this work is noted as the STPN framework, as shown in Fig. 3. When there is only one time-series at the aggregate side (usually the total energy consumption), it is a one-to-one relationship between the total energy consumption, we note it as the PFSA approach, which follows the definition in Section 2.

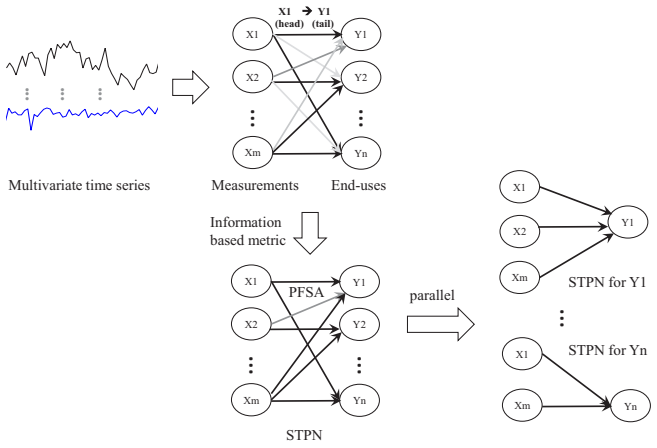

Fig. 3. Formulation of STPN for NILM with multivariate measurements [24]. The multivariate time-series (measurement–V_i and end-use–A_j) are represented as nodes in a graphical model (shown in the top panel), the ability of predicting the end-use from each measurement is estimated via information based metric (e.g., mutual information) based on the formulation of PFSA in Section 2 and Fig. 1. The selected time-series are used in the STPN model (shown in the bottom panel) to learn the disaggregation model. The STPN can be implemented in a parallel manner to improve computational efficiency (shown in the bottom-right panel) where an STPN is formed for the disaggregation of one end-use.

It should be noted that, increasing the number of symbols during partitioning will preserve the more information for disaggregation. However, the larger number of symbols will significantly increase the dimension of the transition matrix, and hence cause difficulty in stability of model learning. Also, due to the use of joint states, the number of states will surge when several variables are considered. A state merging approach is introduced to avoid the above issues. To implement the state merging, states that are less informative are first identified. The metric $\gamma(r)$ to evaluate the importance of the state is defined as,

$$\gamma(r) = \left|\left|Pr(\phi_r, \tau_n^J) - \overline{Pr}(\phi_r, \tau^J)\right|\right|_1, \; r = 1, 2, \cdots, \prod_{\mathbb{A}=1}^{f}|\sigma^{\mathbb{A}}| \tag{2}$$

where

$$\overline{Pr}(\phi_r, \tau^J) = \sum_{n=1}^{\prod_{\mathbb{A}=1}^{g}|\tau^{\mathbb{A}}|} Pr(\phi_r, \tau_n^J) / \prod_{\mathbb{B}=1}^{g}|\tau^{\mathbb{B}}|$$

If $\gamma(r) < \eta$ where η is a specified threshold, the state ϕ_r is identified to be merged to other states. Then the relevance $\Gamma(r, s)$ of the two sates is defined as,

$$\Gamma(r, s) = \sum_{n=1}^{\prod_{\mathbb{B}=1}^{g}|\tau^{\mathbb{B}}|} \left|\left|Pr(\phi_r, \tau_n^J) - Pr(\phi_s, \tau_n^J)\right|\right|_1, \quad r, s = 1, 2, \cdots, \prod_{\mathbb{A}=1}^{f}|\sigma^{\mathbb{A}}| \tag{3}$$

$\Gamma(r, s)$ can be applied to find out the closest state ϕ_s to be merged, where $\gamma(s) \geq \eta$. Also, we can have the states that $\Gamma(r, s) < \mathcal{D}$ to be merged, where the ϕ_r and ϕ_s are the states with very similar transition probabilities, here $\mathcal{D}$ is a specified threshold.

For the end-uses, it can include all of them in one STPN model or several of them which have strong dependency. Also, it can be used for one-by-one disaggregation, where each STPN model is learnt to predict one end-use. If all end-uses are included in the model, the learning process automatically preserves the property such that the sum of the end-use power is equal to the total power consumption. However, when there is a large number of end-uses, the learning process may become computationally expensive.

For the number of multivariate time-series ($\mathbf{X}$) at the aggregate side, tens of variables may be available in different scenarios. The more variables used, the more information is included in the model, while the computational cost is also increased. Here, a mutual information based metric is applied to select the most valuable variable. $\mathbf{X}^u$ is the variables that are currently included in STPN, and $\mathbf{X} \setminus \mathbf{X}^u$ are the candidates can be added into STPN model, the most valuable variable X^e is determined by that the added time-series has the maximal mutual information among all the candidates.

$$X^e = \arg\max\{\Lambda^{(X^u \cup X^e) \to Y}\}, X^e \in \mathbf{X} \setminus \mathbf{X}^u \tag{4}$$

where $\Lambda^{(X^u \cup X^e) \to Y}$ is the mutual information metric of the pattern $(X^u \cup X^e) \to Y$–from the aggregate side (with the newly added variableX^e) to the end-use(s).

4. Case study using mixed types of data in RBSAM data set

1) Data set and problem setup: The Residential Building Stock Assessment data set is collected based on a field

study by Pacific Northwest National Laboratory (PNNL) and Northwest Energy Efficiency Alliance (NEEA) in 2013 [25], [26]. RBSA electric consumption data is based on field data from a representative random sample of existing homes, which encompasses 28-months of 15-minute observations within single-family homes in the Pacific Northwest United States [27].

In addition to whole building electricity use, there are typically 25 sub-metered loads per home including various types of heating, ventilating and air conditioning (HVAC) systems, appliances, lighting, entertainment, home office and plug loads. The Northwest had no precedence for a residential field study of this size and nature of the RBSA, and it was thus a new standard for residential characterization studies in the Northwest. The 2009 International Energy Conservation Code classifies RBSA metered homes in IECC Climate Zones 4, 5, and 6.

In addition to the measured variables, moving average of the whole building electric (WBE) and time of day (ToD) are also used.

During the training, the sub-metered data for each end-use is applied to learn the transition probabilities between the multivariate time-series data. The information based metric is used to select the candidates for disaggregation. The WBE is always used, while the others are chosen by the information based metric. The time periods for training and test are 21 days (e.g. Jun. 1–Jun. 21, 2012, Mar. 1–Mar. 21, 2013) and 7 days (e.g. Jun. 22–Jun. 28, 2012, Mar. 22–Mar. 28, 2013), respectively.

Comparison approaches. Factorial Hidden Markov Model: Factorial Hidden Markov Model (FHMM) [4] is an extension of Hidden Markov Models that parallelizes multiple Markov models in a distributed manner, and performs some task–related inference to arrive at predicted observation. The application of such models is done by representing each end–use as a hidden state that is modeled by multinomial distribution using $\mathbb{K}$ discrete values, and then sum each appliance meter's individual independent contribution to the expected observation (i.e., the total expected main meter value). AFAMAP [9] variant of FHMM which includes the trends in the hidden states of FHMM has also been reported to be effective in the disaggregation task. In our application of FHMM, the number of hidden states is the number of testing appliances, while $\mathbb{K}$ = 3 in order to keep the computational requirements low.

Combinatorial Optimization: Combinatorial optimization (CO) [28] algorithm is a heuristic scheme that attempts to minimize the ℓ_1–norm of the total power at the mains and the sum of the power of the end–uses, given either single or multi–state formulation of the sum. The drawbacks of CO for disaggregation tasks are its sensitivity to transients and degradation with increasing number of devices or similarity in device characteristics.

Metrics for evaluating performance: Here, metrics to evaluate the disaggregation performance in different aspects are applied including root mean square error (RMSE), aggregation error (AE), normalized disaggregation error (NDE).

RMSE for ith end-use is defined as, $\sum_{t=1}^{T}\sqrt{(\hat{y}_t^i - y_t^i)^2}$, where $\hat{y}_t^i$ is the prediction for the ith end-use at tth time step, y_t^i is the ground truth for the ith end-use at tth time step.

AE for the ith end-use is defined as (SAE in [12]), $\text{AE} = \frac{|\sum_{t=1}^{T}\hat{y}_t^i - \sum_{t=1}^{T} y_t^i|}{\sum_{t=1}^{T} y_t^i}$. AE reflects the error of the algorithm in predict the total energy consumption of each end-use in a period of time. NDE for ith end-use is defined as [12], $\text{NDE} = \frac{\sum_{t=1}^{T}(\hat{y}_t^i - y_t^i)^2}{\sum_{t=1}^{T}(y_t^i)^2}$. NDE evaluates the performance of the algorithm for predicting the energy consumption at each time step. Accuracy is defined as [5], $\text{Acc} = 1 - \frac{\sum_{t=1}^{T}\sum_{i=1}^{g}|\hat{y}_t^i - y_t^i|}{2\sum_{t=1}^{T}\sum_{i=1}^{g} y_t^i}$. The accuracy metric estimates the performance of the algorithm in all of the end-uses at all time steps.

2) Selection of informative variables for disaggregation: The information based metric (mutual information) is presented to select the most useful variables for disaggregation. A case study is shown here to analyze the relationship between mutual information metric and the disaggregation performance (RMSE for an end-use is used here). The metered and sub-metered data in 12 months of a home is used. For each month, two variables (WBE plus another one –ODT, IDT, WST, MVG, or ToD) are applied to disaggregate the end-use (in this case, APPL is shown as an example) with the same training and testing scheme. The RMSE and mutual information are plotted in Fig. 4, where the Pearson correlation coefficient between them is -0.88 and p-value is 1.8×10^{-20}. It is therefore concluded that the mutual information metric is negative relative to the disaggregation error (RMSE), which means that applying the variable with higher mutual information of the pattern (from the measured variable to the end-use) will achieve better performance in disaggregation.

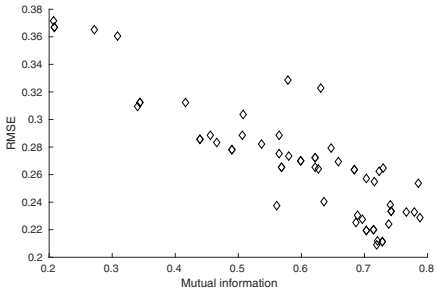

Fig. 4. Relationship between mutual information of the pattern (WBE+?→end-use) and the disaggregation performance. Each point represents a testing case using WBE plus another variable (ODT, IDT, WST, MVG, or ToD)) to predict the end-use (APPL is shown here). The same training and testing scheme is applied in all 12 months' data of the same home.

3) Disaggregation performance with the number of used variables in STPN scheme: With mutual information metric

to select the next measurement for disaggregation, comparisons are carried out between the performance and the number of the variables. The results are shown in Fig. 5, where the HVAC is disaggregated during Mar. 2013. The used variables and the disaggregation performance are listed in Table I.

It can be seen that the disaggregation error decreases with the increasing number variables used. Note that, MVG and ToD are the variables generated without the requirement of additional sensors. In this context, the proposed STPN framework provides us the privilege of improving disaggregation without the requirement of new measurement.

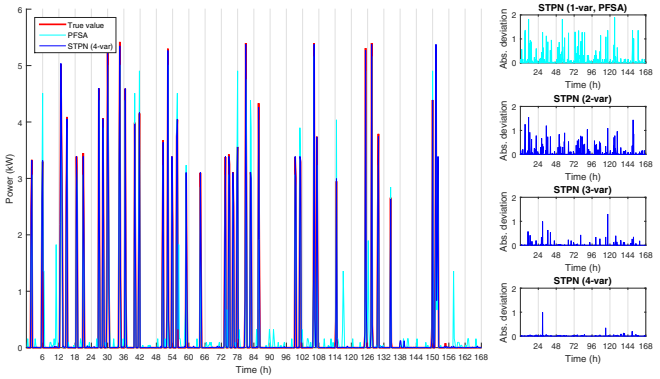

Fig. 5. The disaggregation performance increases with the number of used variables. The HVAC disaggregation of Mar. 22-28, 2013 is shown on the left panel with two methods (PFSA–only WBE is applied, and STPN(4-var)–four variables are used). The absolute errors of the four approaches are shown in the right panel where the used variables increase from one to four.

TABLE I

PERFORMANCE OF STPN WITH INCREASING NUMBER OF VARIABLES USED.

Method	Variables	RMSE	AE	NDE
PFSA	WBE	0.2971	0.0370	0.0691
STPN (2-var)	WBE, MVG	0.2139	0.0015	0.0358
STPN (3-var)	WBE, MVG, IDT	0.0896	0.0018	0.0063
STPN (4-var)	WBE, MVG, IDT, ToD	0.0441	0.0017	0.0015

4) Comparisons to FHMM and CO: The comparisons of the STPN to FHMM and CO are illustrated using the data in Jun. 2013. The disaggregation results and ground truth are shown in Fig. 6. The STPN results are obtained using 3 variables.

It should be noted that, as NILMTK only applies three states for most of the test cases here, the actual disaggregation results don't reflect the true values of the end-uses well. However, the four types of end-uses are combinations of several appliances, the power usage is more than on/off status. This implies that STPN should get better performance in terms of using more states.

FHMM and CO capture the profiles of energy consumption in some appliances (e.g., Fig. 6 (a)–APPL and (b)–HVAC). However, there are considerable errors in the disaggregation, even only looking at the on/off status. From the plots of PFSA (e.g., the third panels of (a) and (d) in Fig. 6), PFSA can capture the on/off status, and the actual values are finer than FHMM and CO, although there are misdisaggregation in quite a few cases. When applying more variables by STPN, the on/off status is well captured as well as the actual values. For the performance, the results of RMSE, AE, NDE, and accuracy are listed in Table II. For home 1, PFSA is better than FHMM and CO, while FHMM gets higher accuracy in home 2 than PFSA and CO. In both homes, STPN outperforms FHMM and CO.

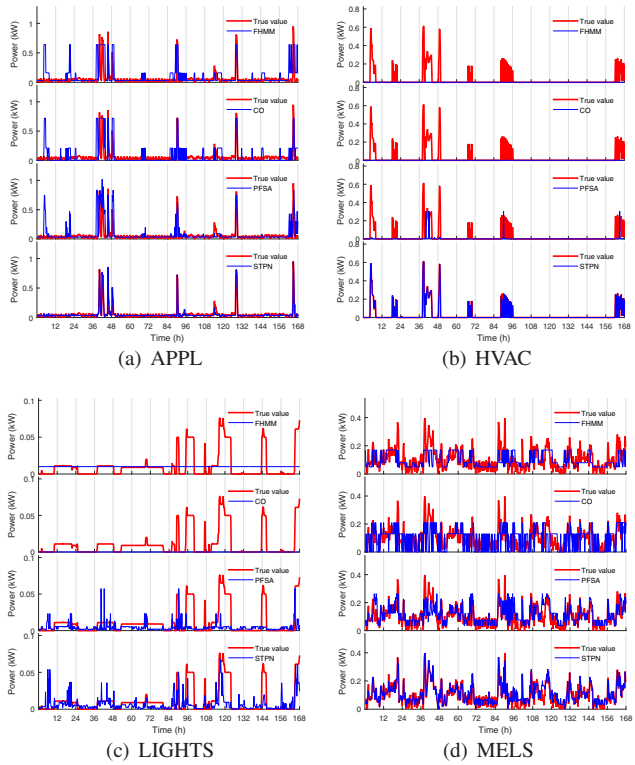

(a) APPL (b) HVAC

(c) LIGHTS (d) MELS

Fig. 6. Disaggregation results using FHMM, CO, PFSA, and STPN using data in Jun. 2013 at home 1.

TABLE II

PERFORMANCE OF PFSA AND STPN WITH COMPARISON TO FHMM AND CO.

ID	FHMM	CO	PFSA	STPN
1/APPL	0.14/0.58/1.17	0.13/0.15/1.04	0.13/0.41/0.96	0.02/0.05/0.03
1/HVAC	0.10/1.00/1.00	0.10/1.00/1.00	0.10/0.92/0.95	0.01/0.01/0.01
1/LIGHTS	0.02/0.06/0.73	0.02/1.00/1.00	0.02/0.60/0.83	0.02/0.37/0.54
1/MELS	0.06/0.07/0.26	0.08/0.09/0.37	0.06/0.11/0.20	0.03/0.06/0.05
1/Acc	0.63	0.58	0.68	0.90
2/APPL	0.16/0.04/0.46	0.24/0.04/0.99	0.35/1.19/2.11	0.04/0.03/0.03
2/HVAC	0.18/0.13/0.19	0.24/0.08/0.36	0.29/0.63/0.50	0.03/0.01/0.01
2/LIGHTS	0.06/0.55/1.31	0.10/2.17/3.79	0.06/0.75/1.14	0.03/0.06/0.39
2/MELS	0.13/0.12/0.13	0.23/0.58/0.42	0.11/0.13/0.09	0.04/0.004/0.01
2/Acc	0.81	0.60	0.68	0.95

*The values of the three metrics (RMSE/AE/NDE) are listed respectively.

5. Conclusions

This work presented a spatiotemporal pattern network (STPN) framework to utilize multivariate time-series data for non-intrusive load monitoring (NILM). The proposed STPN framework is capable of (i) using diverse types of data, (ii) discovering specific patterns of energy usage/generation in phasor measurements, and (iii) energy disaggregation using whole building electric (WBE) consumption and other available concurrent information (e.g., indoor/outdoor temperature, time of day, and move average of WBE).

Future work will pursue: (i) gathering more building and appliance information (RBSAM data set) to enhance the similarity confidence between homes and (ii) cluster analysis in a residential area with the purpose of minimizing the installment cost and maximizing the disaggregation performance.

Acknowledgement

This work was supported by the National Science Foundation under Grant No. CNS-1464279. The authors would like to express their sincere gratitude to Dr. Soumalya Sarkar for the support on the mutual information based metric.

References

[1] M. Zeifman, K. Roth, Non-intrusive appliance load monitoring (NIALM): Review and outlook, 2011, pp. 1–27.

[2] M. Baranski, J. Voss, Genetic algorithm for pattern detection in nialm systems, in: Systems, man and cybernetics, 2004 ieee international conference on, Vol. 4, IEEE, 2004, pp. 3462–3468.

[3] J. Liang, S. K. Ng, G. Kendall, J. W. M. Cheng, Load signature study - part i: Basic concept, structure, and methodology, IEEE Transactions on Power Delivery 25 (2) (2010) 551–553.

[4] Z. Ghahramani, M. I. Jordan, Factorial hidden markov models, Kluwer Academic Publishers, Boston, MA (1997).

[5] J. Z. Kolter, M. J. Johnson, Redd: A public data set for energy disaggregation research, in: Workshop on Data Mining Applications in Sustainability (SIGKDD), San Diego, CA, Vol. 25, 2011, pp. 59–62.

[6] N. Batra, J. Kelly, O. Parson, H. Dutta, W. Knottenbelt, A. Rogers, A. Singh, M. Srivastava, Nilmtk: An open source toolkit for non-intrusive load monitoring, 5th International Conference on Future Energy Systems(ACM e-Energy), Cambridge UK (2014) 1 –14.

[7] K. Anderson, A. Ocneanu, D. Benitez, D. Carlson, A. Rowe, M. Berges, Blued: A fully labeled public dataset for event-based non-intrusive load monitoring research, In Proceedings of 2nd KDD Workshop on Data Mining Applications in sustainability, Beijing, China (2012) 12 –16.

[8] S. Barker, A. Mishra, D. Irwin, E. Cecchet, P.Shenoy, J. Albrecht, Smart*: An open data set and tools for enabling research in sustainable homes, In Proceedings of 2nd KDD Workshop on Data Mining Applications in sustainability, Beijing, China.

[11] O. Parson, S. Ghosh, M. Weal, A. Rogers, Non-intrusive load monitoring using prior models of general appliance types, In Proceedings of the 26th AAAI Conference on Artificial Intelligence , Toronto, ON, Canada (2012) 356 – 362.

[9] J. Z. Kolter, T. Jaakola, Approximate inference in additive factorial hidden markov models with application in energy disaggregation, In Proceedings of the International Conference on Artificial Intelligence and Statistics, La Palma, Canary Islands (2012) 1472 – 1482.

[10] M. J. Johnson, A. S. Willsky, Bayesian nonparametric hidden semi-markov models, Journal of Machine Learning Research 14 (Feb) (2013) 673–701.

[12] M. Zhong, N. Goddard, C. Sutton, Latent bayesian melding for integrating individual and population models, in: C. Cortes, N. D. Lawrence, D. D. Lee, M. Sugiyama, R. Garnett (Eds.), Advances in Neural Information Processing Systems 28, Curran Associates, Inc., 2015, pp. 3618–3626.

[13] G. C. Koutitas, L. Tassiulas, Low cost disaggregation of smart meter sensor data, IEEE Sensors Jounal 16 (6) (2015) 1665–1675.

[14] J. Kelly, W. Knottenbelt, Neural nilm: Deep neural networks applied to energy disaggregation, Proceedings of 2nd ACM International Conference on Embedded Systems for Energy-Efficient Built Environment - Buildsys'15 (2015) 55–64.

[15] H. Shao, M. Marwah, N. Ramakrishnan, A temporal motif mining approcah to unsupervised energy disaggregation applications to residential and commercial buildings, 1st International Workshop on Non-Intrusive Load Monitoring (2012) 1 – 7.

[16] S. Giri, M. Berges, An energy estimation framework for event-based methods in non-intrusive load monitoring, Elsevier Journal of Energy Conversion and Management 90 (2015) 488 – 498.

[17] S. M. Tabatabaei, S. Dick, W. Xu, Toward non-intrusive load monitoring via multi-label classification, IEEE Transactions on Smart Grid 8 (1) (2017) 26–40.

[18] J. M. Gillis, S. M. Alshareef, W. G. Morsi, Nonintrusive load monitoring using wavelet design and machine learning, IEEE Transactions on Smart Grid 7 (1) (2016) 320–328.

[19] Z. Jiang, C. Liu, A. Akintayo, G. Henze, S. Sarkar, Energy prediction using spatiotemporal pattern networks, arXiv preprint arXiv:1702.01125.

[20] C. Liu, S. Ghosal, Z. Jiang, S. Sarkar, An unsupervised spatiotemporal graphical modeling approach to anomaly detection in distributed cps, in: Proceedings of the International Conference of Cyber-Physical Systems, (Vienna, Austria), 2016.

[21] C. Liu, S. Ghosal, Z. Jiang, S. Sarkar, An unsupervised anomaly detection approach using energy-based spatiotemporal graphical modeling, Cyber-Physical Systems (2017) 1–37.

[22] C. Rao, A. Ray, S. Sarkar, M. Yasar, Review and comparative evaluation of symbolic dynamic filtering for detection of anomaly patterns, Signal, Image and Video Processing 3 (2) (2009) 101–114.

[23] S. Sarkar, S. Sarkar, N. Virani, A. Ray, M. Yasar, Sensor fusion for fault detection and classification in distributed physical processes, Frontiers in Robotics and AI 1 (2014) 16.

[24] C. Liu, A. Akintayo, Z. Jiang, G. P. Henze, S. Sarkar, Multivariate exploration of non-intrusive load monitoring via spatiotemporal pattern network, Applied Energy 211 (2018) 1106–1122.

[25] D. Baylon, P. Storm, K. Geraghty, B. Davis, Residential building stock assessment: single-family characteristics and energy use, Northwest Energy Efficiency Alliance.

[26] E. Mayhorn, G. Sullivan, R. Butner, H. Hao, M. Baechler, Characteristics and performance of existing load disaggregation technologies, PNNL-24230.

[27] N. E. E. Alliance, Residential building stock assessment: Metering study, Tech. rep., Report (2014).

[28] J. C. William, H. C. William, R. P. William, A. SCHRIJVER, Combinatorial Optimization, 5th Edition, Vol. 21, Springer, 2011.